Sodium Diisopropylamide:

## Aggregation, Solvation, and Stability

Russell F. Algera, **Yun Ma**, and **David B. Collum**[*]

Department of Chemistry and Chemical Biology, Baker Laboratory, Cornell University, Ithaca, New York 14853–1301, United States, dbc6@cornell.edu

Abstract

The solution structure, stabilities, physical properties, and reactivities of sodium diisopropylamide (NaDA) in a variety of coordinating solvents are described. NaDA is stable for months as a solid or as a 1.0 M solution in *N,N*-dimethylethylamine (DMEA) at −20 °C. A combination of NMR spectroscopic and computational studies show that NaDA is a disolvated symmetric dimer in DMEA, *N,N*-dimethyl-*n*-butylamine, and *N*-methylpyrrolidine. Tetrahydrofuran (THF) readily displaces DMEA, affording a tetrasolvated cyclic dimer at all THF concentrations. Dimethoxyethane (DME) and *N,N,N′,N′*-tetramethylethylenediamine (TMEDA) quantitatively displace DMEA, affording doubly chelated symmetric dimers. The trifunctional ligands *N,N,N′,N″,N″*-pentamethyldiethylenetriamine and diglyme bind the dimer as bidentate rather than tridentate ligands. Relative rates of solvent decompositions are reported, and rate studies for the decomposition of THF and DME are consistent with monomer-based mechanisms.

TOC Graphic
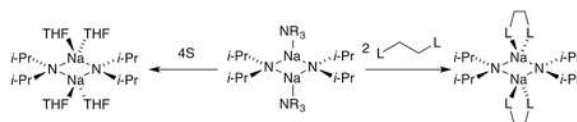
Introduction

Several groups, most recently that of Mulvey, have underscored the merits of sodium dialkylamides,[1,2] but the response of the synthetic organic community remains muted compared with the enthusiastic embrace of lithium diisopropylamide (LDA) and related lithium dialkylamides.[3] Sodium diisopropylamide (NaDA) is an excellent case in point. Since the initial preparation of NaDA by Levine in 1959[4] and subsequent improved preparations,[5] NaDA has languished in relative obscurity, appearing in the literature only a dozen times over half a century.[6] This scarcity is somewhat perplexing on first inspection. NaDA is easily prepared, stable as a solid if refrigerated, and a powerful Brønsted base.[5,6]
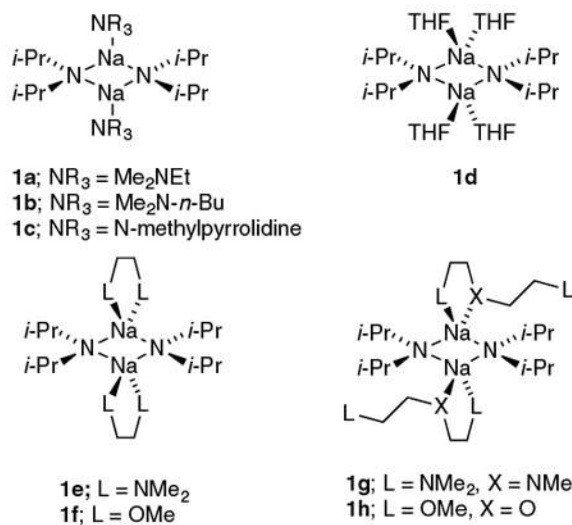
[*]David B. Collum dbc6@cornell.edu.

The authors declare no competing financial interests.

We surmised that potential users must be leery of the rapid destruction of standard ethereal solvents by NaDA and its insolubility in inert hydrocarbons. In short, NaDA is inconvenient.

In our first paper of this series, we reported that 1.0 M solutions of NaDA in neat *N,N*-dimethylethylamine (DMEA) or DMEA–hydrocarbon mixtures are stable for weeks at room temperature and for months under refrigeration.[7] Moreover, NaDA–DMEA can be prepared in 15 min from technical-grade reagents without pre-purification or pre-drying. Metalations of a dozen substrates with a broad range of functionality have shown that NaDA–DMEA is often orders of magnitude more reactive than LDA–THF toward orthometalations, dehydrohalogenations, diene metalations, and epoxide eliminations.[7] The stereo- and chemoselectivities of the two bases are also complementary. Even concerns that the sodiated intermediates and products in DMEA might be insoluble have proved unfounded. Overall, the results of our initial studies were highly encouraging, and, as a referee noted, "running reactions in trialkylamine solvent is not crazy."

1a; NR$_3$ = Me$_2$NEt
1b; NR$_3$ = Me$_2$N-*n*-Bu
1c; NR$_3$ = N-methylpyrrolidine

1d

1e; L = NMe$_2$
1f; L = OMe

1g; L = NMe$_2$, X = NMe
1h; L = OMe, X = O

In this second paper, we examine the solution structure and stability of NaDA solvated by DMEA, other trialkylamines, and a number of synthetically important coordinating ligands including tetrahydrofuran (THF), *N,N,N′,N′*-tetramethylethylenediamine (TMEDA), and 1,2-dimethoxyethane (DME). The cyclic dimer motif (**1a–h**) is the only detectable form. DMEA is substitutionally labile, which is a critical prerequisite for the addition of other ligands before metalation to modulate the reactivity of NaDA and after metalation to control reactivity of the resulting sodium salts. Mechanistic studies of solvent decomposition offer the first glimpse into NaDA reactivity. This paper is intended to detail the structural foundations underpinning NaDA structure–reactivity–selectivity principles of potential interest to synthetic organic chemists.

Results

Methods.

We modified the dissolving metal method first described by Wakefield and co-workers[5a] by using kinetically inert and solubilizing DMEA as the bulk solvent.[5,7] Although the procedure affords 1.0 M stock solutions of NaDA adequate for synthetic applications, a precautionary crystallization from DMEA–hexane was included for spectroscopic and rate studies. We hasten to add that the typical user will detect little or no difference between the pre- and post-purified reagent.

Given the absence of resolved ^{23}Na–^{15}N coupling owing to the quadrupolar ^{23}Na nucleus and with an eye toward expanding the application of the method of continuous variations (MCV) to aggregated organometallic species lacking NMR-active metal nuclei, we turned to MCV to assign the solution structure.[8,9] In short, an ensemble generated from constitutionally similar species of unknown aggregation number (A_n and B_n, eq 1) is monitored with NMR spectroscopy as a function of mole fraction X_A or X_B. The number of heteroaggregates attests to the aggregation state. Plotting the relative proportions versus mole fraction affords a Job plot confirming the assignment.

$$A_n + B_n \rightleftharpoons A_n + A_{n-1}B_1 + A_{n-2}B_2 + \ldots + B_n \quad (1)$$
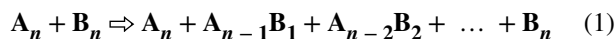
For this study, NaDA was paired with sodium dicyclohexylamide (NaDCA)[5c,10] and sodium isopropylcyclohexylamide (NaICA).[9a] NaICA was previously suggested to be dimeric, as evidenced by two stereoisomers (*cis*-**2** and *trans*-**2**, eq 2; Cy = cyclohexyl).[9a] We confirmed the dimer assignment for NaICA and showed that both NaDA and NaDCA are dimers **1** and **3**, respectively, by examining NaDA–NaICA and NaDA–NaDCA mixtures using ^{13}C and ^{15}N NMR spectroscopies. NaDA–NaDCA pairings are superior and are emphasized below. Considerable data for the NaDA–NaICA pairings are archived in the supporting information. Although ^{1}H NMR spectroscopy proved especially valuable in MCV-based studies of sodium enolates,[9a,11] the resolution was inadequate for the study of sodium dialkylamide aggregation.


(2)

$$S_n$$
Cy,,,N—Na—N,,,Cy
Cy—N Na N—Cy
$$S_n$$

3
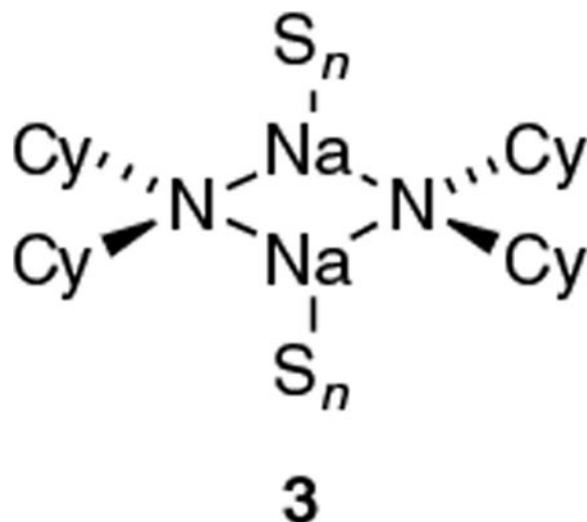
The strategies and quantitative insights into solution solvation numbers of NaDA are notable in our opinions. Confirmations and experimentally elusive details are provided with density functional theory (DFT) computations at the B3LYP/6–31G(d) level,[12] with single-point calculations at the MP2 level of theory.[13]

Solution Structure: NaDA in DMEA and related amines.

^{13}C NMR spectra of NaDA–NaDCA mixtures in DMEA showed the dimer ensemble depicted in eq 3 with resolution of all ^{13}C methine resonances of the isopropyl and cyclohexyl moieties (Figure 1a). A plot of the relative integrations of **1**, **3**, and **4** afforded the Job plot illustrated in Figure 2, which is characteristic of statistically distributed dimers.
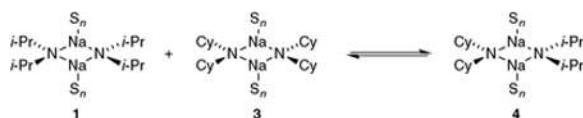
(3)

A ^{15}N NMR spectrum of a 1:1 mixture of [^{15}N]NaDA and [^{15}N]NaDCA shows signals corresponding to two homodimers and a heterodimer distributed statistically (Figure 1b). A Job plot based on ^{15}N NMR data is analogous to that shown in Figure 2 (supporting information).

MCV analyses using the NaDA–NaICA mixtures (eq 4) were effective, but they have been largely relegated to supporting information. Several interesting observations are worth noting, however. The ^{13}C NMR data resolved two methinyl resonances in each of the two NaICA homodimers as well as the four methinyl resonances in heterodimer **5** (eq 2), readily affording the corresponding Job plot. ^{15}N NMR spectroscopy using [^{15}N]NaDA and [^{15}N]NaICA showed that the ^{15}N resonances of the homo- and heteroaggregated NaICA

fragments are poorly resolved, whereas homo- and heteroaggregated NaDA fragments are well-resolved. Poor resolution on one pair is not critical;[9a] the resulting Job plot is consistent with a statistical distribution of dimers.
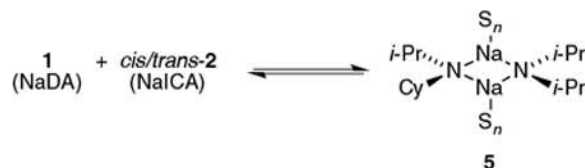
(4)

^{13}C and ^{15}N NMR spectroscopic investigations of the NaDA–NaDCA pair in *N,N*-dimethylbutylamine (DMBA) and *N*-methylpyrrolidine showed that NaDA is dimeric (supporting information). DFT computations showed that sequential solvation of dimeric NaDA by DMEA is highly exothermic and affords disolvate **1a**, but no minima corresponding to tri- or tetrasolvated dimers were found. The sterically less demanding and computationally simpler Me_3N gave similar results. This outcome contrasts sharply with ethereal and multidentate ligands (*vide infra*).


1a
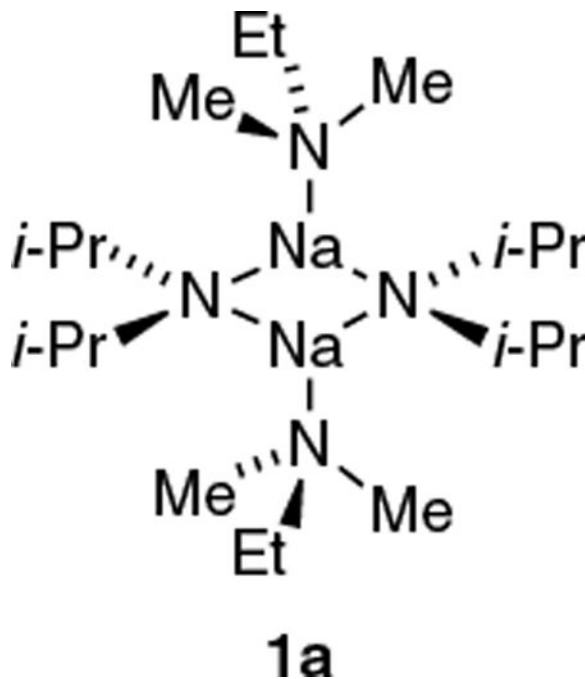
Owing to our experience with DFT computations in lithium chemistry, we were comfortable with the assignment of **1a** as disolvated. Nonetheless, we applied several experimental methods to determine the solvation as follows. Proton diffusion-ordered NMR spectroscopy ([1]H-DOSY), first applied to organolithium aggregates by Williard,[15] is now proliferating

within the field[16] and has been applied to organosodiums.[17] Underlying assumptions about molecular shape and influence on the diffusion constant have always left us uneasy, however.

We examined the structure of NaDA in DMEA using the double bipolar pulse pair stimulated echo sequence with convection compensation pulse sequence to measure the diffusion coefficients of NaDA dissolved in DMEA. An analogous experiment independently measured diffusion coefficients for DMEA, THF, tetramethylsilane, anisole, 1,3-dimethoxybenzene, and 18-crown-6 to obtain the molecular weights for NaDA shown in Table 2. Although the data recorded at ambient temperature seemed to confirm the disolvated dimer, the molecular weight at −80 °C was 30% low. Similar temperature dependencies have been noted by others.[16,17] We have no evidence, however, that the reduced value at −80 °C is based on a structural change: low temperature promotes rather than retards solvation owing to negative enthalpy. Also, the solubility of NaDA in DMEA is nearly temperature-independent. The results from THF solvate **1f** (see Table 1) are discussed below.

A more traditional probe of solubility provided significant insight.[18] The concentration of DMEA-solubilized NaDA in a suspension of NaDA in toluene-d_8 was monitored as a function of added DMEA using ^{1}H NMR spectroscopy and benzene as an internal standard; the two-phase equilibrium is described in eq 5.[19] If DMEA coordinates to and solubilizes NaDA quantitatively ($K_{solv} \gg 1$), the concentration of NaDA will be proportional to the concentration of DMEA until full solubility is achieved, with the solvation number being extractable from the slope and the endpoint (eq 8). We see this behavior for superior solvents (*vide infra*). In the limit of weak binding ($K_{solv} \ll 1$), the solubility will be low while manifesting curvature diagnostic of the coordination number (eq 9). The measured concentration of NaDA in solution versus added DMEA (Figure 3) showed non-limiting behavior: it is upwardly curving with a fit to eq 7 showing disolvated dimer ($n = 2$). Forcing the model to a tetrasolvated dimer ($n = 4$) provided a markedly inferior fit to the data.

$$(A)_{solid} + nS \overset{K_{solv}}{\rightleftharpoons} (A_2S_n)_{solution} \quad (5)$$
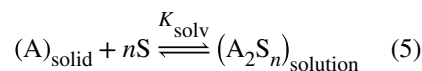
$$K_{solv} = [A_2S_n]/[S]^n \quad (6)$$

$$[A_2S_n] = K_{solv}([S]_0 - n[A_2S_n])^n \quad (7)$$

$$[A_2S_n] = [S]_0/n \quad (8)$$

$$[A_2S_n] = K_{solv}[S]_0^n \quad (9)$$

Thus, recalcitrant solubilization of NaDA by DMEA reflects weak binding. This notion is reinforced by studies of additional monodentate trialkylamines (supporting information). As steric demands increase, the binding constant, K_{solv}, decreases. The poor solubility of NaDA in triethylamine, for example, stems from weak coordination rather than a low solubility of the doubly solvated dimer. We return to this idea in the discussion.

Solution Structure: NaDA–THF.

MCV using ^{13}C and ^{15}N NMR spectroscopies for NaDA–NaICA and NaDA–NaDCA pairs demonstrated that THF-solvated NaDA is dimeric at both low and high THF concentrations (supporting information). As usual, determining the solvation state demanded several strategies. Incremental additions of THF to NaDA in 2.0 M DMEA (Figure 4) showed clear saturation of the changing chemical shifts of the methine proton and ^{15}N resonances resulting from ligand substitution consistent with strongly preferential THF coordination. However, curvature with saturation occurring at ≈3.0 equiv of THF per sodium (as opposed to a linear dependence with a sharp endpoint) belied non-quantitative substitution, thereby obscuring the stoichiometry. Fortunately, titration of a suspension of NaDA in toluene, as described for trialkylamines (Figure 5 and eqs 5–7), revealed a linear dependence of the measured titer on added THF and a constant 2:1 THF/NaDA ratio in solution up to full solubilization at 2.0 equiv. This outcome is fully consistent with tetrasolvate **1f**.

The tetrasolvated form is also strongly supported computationally (eq 10). Given the exothermicity and our experience that DFT computations tend to falter with congested systems, we are confident in the tetrasolvate assignment.
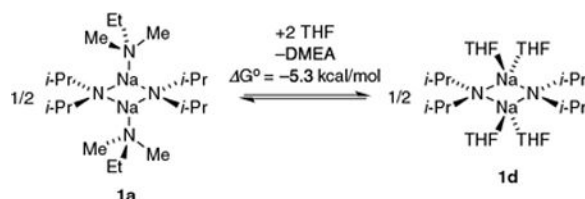
$$(10)$$

Solution Structure: NaDA–TMEDA.

MCV showed that the solution aggregation state of NaDA–TMEDA is akin to the reported doubly chelated crystal structure (supporting information).[6b] We hoped to observe free and bound TMEDA in the slow-exchange limit to directly measure the number of ligands on the bound form, but the exchange was rapid at −100 °C. Two titration methods showed strong coordination by TMEDA and supported a 1:1 proportion of NaDA/TMEDA:

(1) Substitution of DMEA by TMEDA was evidenced by a downfield shift of the methinyl ^{1}H resonance and an upfield shift of the ^{15}N resonance after substitution of TMEDA by DMEA. As found for THF, however, the stoichiometry of the substitution was obscured by non-quantitative binding (supporting information).[19]

(2) Titration of a suspension of NaDA with TMEDA (analogous to that in Figure 5) showed a linear dependence of the measured titer on TMEDA concentration, a constant 1:1 proportion of TMEDA to NaDA in solution up to complete dissolution, and a hard solubility endpoint corresponding to 1:1 stoichiometry of TMEDA/NaDA.

DFT computations showed that the displacement of DMEA by chelated TMEDA (eq 11) is exothermic. This result contrasts with that observed with LDA, which forms a weakly ligated η^1-TMEDA-solvated dimer in solution.[21,22,23]

(11)

Solution Structure: NaDA–DME.

DME acts as an ethereal analog of TMEDA in every respect: (1) ^{13}C NMR spectroscopy in conjunction with MCV showed dimers, (2) incremental addition (akin to those in Figure 5) to NaDA–DMEA showed semi-quantitative binding consistent with one DME per sodium, (3) titration of a NaDA suspension showed a linear dependence of the titer on DME with a hard solubility endpoint at 1:1 stoichiometry, and (4) DFT computations supported a highly exothermic substitution of DMEA by DME *without MP2 correction*. We encountered a unique situation in which uncorrected numbers and geometries corroborated experiment, yet MP2 correction provided highly questionable 1.6 kcal/mol/Na solvation energies (eq 11) for reasons we failed to identify. We explored a variety of larger basis sets with no obvious improvements. All evidence, including the results of experimental competition studies, suggested that the MP2 correction is indeed spurious.

Doubly chelated dimer **1e** contrasts with LDA, in which two DMEs coordinated to the dimer are unchelated.[21,24,25] We also competed TMEDA and DME by swapping one for the other at a fixed total ligand concentration corresponding to 2.0 equiv per sodium and monitored the chemical shifts of the time-averaged free and bound ligand. TMEDA is the stronger ligand by approximately 10-fold.

Solution Structure: NaDA with Other Ligands.

The results of ^{15}N NMR spectroscopy and MCV showed that trifunctional ligands diglyme and *N,N,N′,N″,N″*-pentamethyldiethylenetriamine (PMDTA) are dimers rather than monomers that could have arisen from tridentate ligation. Their binding affinities slightly greater than those of the bidentate analogs DME and TMEDA were commensurate with only a statistical advantage. Thus, these potentially tridentate ligands function as bidentate ligands, as demonstrated by **1g** and **1h**.[26,27] Computations suggest that the third ligand, although not coordinated to sodium as evidenced by long Na–OMe and Na–NMe$_2$ bonds, display distinct preferences for orienting the lone pairs toward the sodium nuclei. We discuss the potential synthetic importance of bidentate rather than tridentate coordination below.

We carried out a brief survey of a number of ligands that lacked rigor but provided useful data nonetheless.[28] Ethereal ligands such as Et$_2$O and 2,5-dimethyltetrahydrofuran substitute for DMEA but much more reluctantly than does THF as expected from binding measurements on lithium amides.[23,26,27] Titration of NaDA/toluene suspensions with anisole displays chemical shift perturbations consistent with binding but no appreciable solubilization, suggesting that anisole is a poor ligand for sodium. The highly dipolar ligand *N,N′*-dimethylpropyleneurea (DMPU) is quickly metalated by NaDA at −80 °C, as evidenced by the rapid appearance of extraneous resonances and diisopropylamine observable with ^{1}H and ^{15}N NMR spectroscopies. The products of these decompositions have not been pursued.[29]

## Solvent Decomposition: Products, Rates, and Mechanisms.[30,31]

Whether in DMEA or in its solid form, NaDA at room temperature has a half-life of approximately two months, consistent with the thermal sensitivity noted by Wakefield.[5b] This decomposition is mitigated by storage at −20 °C in a standard laboratory freezer. However, facile decompositions of DME and DMPU underscore the possible limitations of NaDA when used in conjunction with standard ethereal solvents. The stability of NaDA in selected solvents at room temperature is illustrated in Table 2.

THF decomposition offered our first view of the mechanism of NaDA-mediated metalations. NaDA decomposition in THF–hexane mixtures at 25 °C forms partially soluble *cis* and *trans* alkoxides **7** observable with ^{1}H NMR spectroscopy (Scheme 1). Quenching afforded known alcohols **8** and **9** in the proportions shown in Scheme 1. The presumed intermediate salt **6** is observed at low (equilibrium) levels owing to facile NaDA-mediated isomerization to **7**; the isomerization of **6** under the reaction conditions was confirmed by adding **8** to NaDA–THF-*d*$_8$.

Monitoring the rate of THF decomposition by tracking the loss of **1d** (δ3.11 ppm in ^{1}H NMR) and the formation of diisopropylamine showed that the reaction does not follow a first-order decay, which indicated that the decomposition does *not* occur from the observable dimer. Fitting the traces to the nonlinear Noyes equation[32] afforded an average order of 0.68 (Figure 6), approximating a half order. Plotting initial rates versus THF concentration revealed a second-order THF dependence (Figure 7). The half-order rate constants are nearly independent of the NaDA concentration, albeit with a slight upward drift (Figure 8). The

idealized rate law[33] (eq 12) is consistent with the mechanism described in eq 13.[34] Rate-limiting proton transfer was evidenced by a substantial kinetic isotope effect determined by comparing THF to THF-d_8 ($k_H/k_D = 6.9$).

$$d[A_2(THF)_4]/dt = k[A_2(THF)_4]^{1/2}[THF]^2 \quad (12)$$

$$1/2\ A_2(THF)_4 +\ 2\ THF \xrightarrow{k} [A(THF)_4]^{\ddagger} \quad (13)$$
$$(\textbf{1d})$$
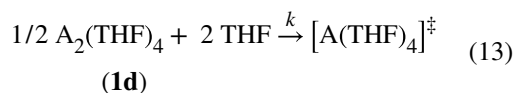
The $[AS_4]^{\ddagger}$ stoichiometry is consistent with an α deprotonation via transition structure **11**–α to generate oxacarbenoid **12** as a precursor to carbene **13** (Scheme 2).[35] Alternatively, a β metalation whether via a concerted E2-like elimination or **11**-β discrete carbanion **14** with post-rate-limiting elimination to **6a** is plausible. Although the isomerization and consequent scrambling dissuaded us from sophisticated isotopic labeling studies, we collected evidence supporting the carbenoid pathway. Comparing THF to THF-d_4 (**15**)[36] afforded $k_H/k_D \sim 6$ suggesting a rate limiting C-H(D) cleavage at the 3 position, but it does not distinguish the two possible mechanisms. Monitoring a mixture of NaDA, THF, and i-Pr$_2$ND by ^{1}H and ^{2}H NMR spectroscopies shows isotopic exchange at the α protons of THF, consistent with α deprotonation. The comparable rates of exchange and decomposition suggest that neither metalation nor insertion are dominantly rate limiting. The existence of discrete carbene **13**, however, is not even assured.


15
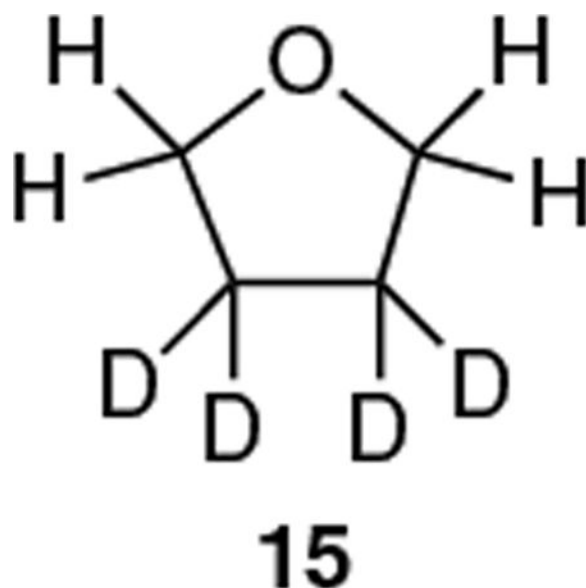
NaDA in DME–toluene undergoes decomposition to give methyl vinyl ether and sodium methoxide (eq 14). Following the proton resonance of **1e** at δ1.10 ppm shows that the decay approximates a half-order rather than a first-order decay (akin to Figure 6). Fitting multiple decays to the nonlinear Noyes equation[32] to ascertain the order by best fit affords an average order of 0.52. Plotting the half-order rate constants versus NaDA concentration showed some upward drift (akin to that in Figure 7). A plot of k_{obsd} versus DME concentration approximated first order with a slight upward curvature (Figure 9), possibly hinting at either low contributions from a more highly solvent-dependent pathway or more generalized medium effects. The structure of **1e** in conjunction with the idealized[33] rate law (eq 15) afforded the generic mechanism in eq 16. The doubly solvated monomer-based transition state, $[A(DME)_2]^{\ddagger}$, is isostructural to THF-based **11** when ligand hapticity is considered. Although DFT computations showed **16** and **17** to be computationally viable, **16** was preferred by ~21 kcal/mol. The low coordination number—the absence of a $^+Na(DME)_3$ fragment[37]—argues against a free-ion-based mechanism.

$$\text{(14)}$$

$$-d[A_2(DME)_2]/dt = k[A_2(DME)_2]^{1/2}[DME]^1 \quad (15)$$

$$1/2\ A_2(DME)_2 +\ DME \rightarrow\ [A(DME)_2]^{\ddagger} \quad (16)$$
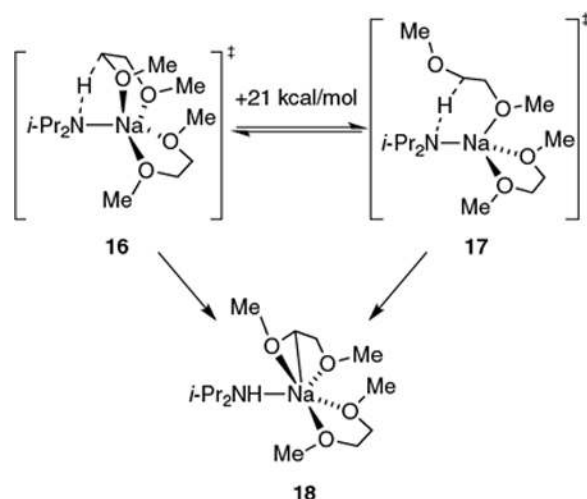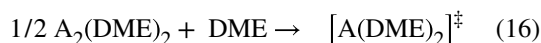
$$\text{(17)}$$

Discussion

The first paper in this series showed NaDA is a highly efficacious Brønsted base when compared with LDA. Our seemingly trivial but potentially consequential contribution at the outset was to show that NaDA is soluble and stable in DMEA and related minimally hindered trialkylamines. We previously asserted that simple trialkylamines have been largely overlooked as ligands for lithium salts, an oversight we attribute to the unfortunate urge to use them in concert with—rather than to the exclusion of—strongly coordinating ethereal ligands.[38]

The structural studies described in this second paper lay foundations for subsequent studies that will dovetail synthetic organic applications with mechanistic investigations. We must suppress the almost irresistible urge to rely on analogy to lithium amides. Parallel behaviors exist, but such analogies are imperfect and demand, at a minimum, experimental support.

Structures.

A survey of NaDA reveals cyclic dimers in solutions containing a number of standard coordinating ligands, analogous to the dominance of LDA dimers (Scheme 3).[21] Even the smallest trialkylamines are so sterically demanding as to afford disolvated dimers of NaDA (**1a**–**1c**) akin to those of LDA. Compared with lithium, however, the larger sodium can accommodate more ligands. LDA dimer, for example, *never* exceeds one solvent per lithium in the solid[39] or solution state[21] (see **19**) and is trisolvated endothermically by THF in silico. [40] Even bifunctional ligands such as DME and TMEDA remain unchelated on the LDA dimer (**20**).[21] By contrast, NaDA in THF forms tetrasolvated dimer **1f**, and both DME and TMEDA readily chelate dimeric NaDA (**1d** and **1e**).[6b] All substitute DMEA exothermically (see eqs 6 and 7).

Comments on Methods.

We use a combination of tactics to understand structure–reactivity relationships and develop new strategies whenever possible. MCV as a method to study aggregation, for example, has its origins in early work from several laboratories[11] and has been of enormous importance to us for studying aggregation in systems in which M–X coupling is not observable.[8,9] To this end, our expansion of the method to include ^{13}C and ^{15}N as observable nuclei is new and noteworthy.

We also explored DOSY as a means to ascertain the structure of NaDA using functional molecular weights as a proxy. DOSY is increasingly popular,[15,16,17] and our results could be considered supportive. That said, however, we remain cautious owing to significant (up to 30%) temperature-dependent changes in measured molecular weights that do not appear to derive from changes in structure.

Solvent Decomposition.

We investigated the decomposition of THF and DME to understand the limitations of standard ethereal solvents as ligands for NaDA (Table 2) and get a first peek at the mechanism of NaDA-mediated metalations. THF decomposition occurred via tetrasolvated-
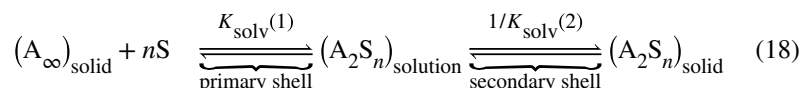
monomer-based α-elimination (**11**). Although isotope effects show rate-limiting cleavage of the C-H(D) bonds at the β position (Scheme 2), unambiguous differentiation of a carbene-derived α-elimination (**11**-α) rather an E2-like β-metalation (**11**-β) was elusive owing to isotopic scrambling. From a synthetic organic (applications) perspective, the high solvent order shows that decomposition can be suppressed by using low ethereal ligand concentrations. Analogous rate suppression allows LDA/THF/hydrocarbon solutions to be sold commercially.

Facile decomposition of DME (eq 12) proceeded via a disolvated-monomer-based transition structure. Both **16** and **17** are computationally viable, with **16** energetically preferred. The suppression of decomposition at low DME concentrations is especially crucial if DME is to find a niche given its lability and relatively high cost (see Table 2).

Thoughts on Solubilities.

One might argue that our interest in the solubilities of NaDA in trialkylamines is excessive, but applications of NaDA–R_3N mixtures are predicated on the fact that high-molarity stock solutions are easily prepared, handled, and stored. Sodiated intermediates must also be soluble to be of value to synthetic chemists. There is, however, a previously undisclosed and subtle motivation for confirming NaDA solubility: ongoing rate studies of NaDA-mediated metalations in trialkylamines display odd rate behaviors that we cannot reconcile easily. Such discussions are beyond the scope of this paper but add to our obsession.

The solubility studies underscored some basic principles of alkali metal salt solubilities that, although not unprecedented, warrant further discussion. NaDA is highly soluble in DMEA and DMEA–hexane yet poorly soluble in triethylamine and TMEDA–hexane at low temperatures: why? This question is nuanced and is summarized in eq 18.

$$\left(A_\infty\right)_{solid} + nS \underset{\text{primary shell}}{\overset{K_{solv}(1)}{\rightleftharpoons}} \left(A_2S_n\right)_{solution} \underset{\text{secondary shell}}{\overset{1/K_{solv}(2)}{\rightleftharpoons}} \left(A_2S_n\right)_{solid} \quad (18)$$

Dissolving unsolvated solid NaDA, denoted as $(A_\infty)_{solid}$, to form solubilized disolvated dimer stems largely from the enthalpy of primary shell solvation:[41,42] the ligand must bind strongly enough to overcome the enthalpy of lattice deaggregation. The fact that the solubility of NaDA in trialkylamines is nearly temperature-independent shows that the two large enthalpic contributions cancel. The overall high solubility shows that $(A_2S_n)_{solution}$ is favorable relative $(A_2S_n)_{solid}$ and $(A_\infty)_{solid}$. Triethylamine, on the other hand, does not bind well; the poor solubility of NaDA correlates with a small binding constant, $K_{solv}(1)$, rather than an inherent insolubility of A_2S_n reflected in $K_{solv}(2)$. The failure of primary shell solvation causes the insolubility of NaDA in triethylamine.

By contrast, TMEDA binds strongly: $K_{solv}(1)$ is large. However, doubly chelated dimer **1d** (A_2S_n in eq 13) has limited solubility at low temperature. Therefore, to the extent that A_2S_n (and almost every organic molecule) is more soluble at high temperature, the solubilization

of $(A_2S_n)_{solid}$ dimer is entropy-dominated.[43] The failure of secondary shell solvation causes the insolubility of NaDA in TMEDA–hexane.

Synthetic Implications.

In our first contribution,[7] we emphasized the merits of NaDA–DMEA for metalations owing to its ease of handling and resistance to base-mediated solvent decomposition.[30,31] However, the substitutional lability of trialkylamines is also synthetically important. In forthcoming papers, we will explore the effects of ethereal ligand additions to NaDA–DMEA mixtures. Ongoing studies show that THF elicits large accelerations relative to that of NaDA–DMEA while the metalation rate far exceeds the THF decomposition rate. The short half-life of NaDA in ethereal stock solutions by no means precludes their use as additives. Mono- and difunctional ethers readily displace coordinated DMEA in NaDA–DMEA stock solutions. Moreover, when robust trialkylamines are required to force a recalcitrant metalation, the resulting salts—arylsodiums, for example—can be treated with ethereal ligands after the metalation to modulate their reactivities. Again, the ligand substitution will be highly favorable.

Hemilabile Trifunctional Ligands.

Trifunctional PMDTA and diglyme afford dimeric NaDA bound only as bidentate ligands (**1g** and **1h**). This outcome segues to a topic of long-standing interest: hemilabile ligands.[44] In contrast to transition metal chemists attempting to build weakly chelating di- and polyfunctional ligands that readily liberate coordination sites,[45] we approach hemilability by identifying ligands that chelate selectively in the transition state to optimize accelerations.[44] Imagine, for example, transformations in which fleeting intermediates bearing a trifunctional ligand (eq 14) are markedly accelerated by transition-state stabilization that is *not* offset by ground-state stabilization. The reader might also realize that we have evidence to support this notion.

1g; L = NMe₂, X = NMe
1h; L = OMe, X = O
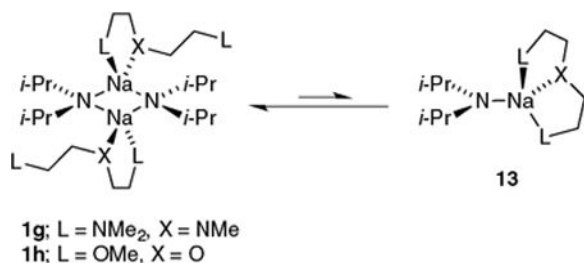
(19)

Conclusions

We are enthusiastic about the promise of NaDA–DMEA mixtures to solve metalation problems that plague synthetic chemists. NaDA is both convenient and demonstrably effective. It can be prepared in minutes using standard glassware and stored for months with refrigeration as 1.0 M DMEA solutions. Metalation rates are typically orders of magnitude

higher than those for LDA–THF.[7] The obvious limitations include the higher costs and unpleasant odors of trialkylamines, but neither precludes application to difficult metalations. Another point that should not be overlooked is that DMEA is substitutionally labile. Stronger ligands, even potentially expensive ligands, can be added *before* the metalation to accelerate it—they do—or *after* the metalation to modulate the reactivity of the resulting sodiated intermediate. Furthermore, quite unlike LDA, NaDA shows little tendency to form mixed aggregates.[21] We are encouraged by the well-defined aggregation and solvation states described herein that are required to unravel the mechanistic details of NaDA-mediated metalations and correlate them with selectivities.

Experimental

Reagents and solvents.

THF, DME, diethyl ether, TMEDA, PMDTA, diglyme, hexane, and all trialkylamines were distilled from blue or purple solutions containing sodium benzophenone ketyl. [^{15}N]diisopropylamine,[46] [^{15}N]dicyclohexylamine,[47] and [^{15}N]isopropylcyclohexylamine[48] have been described previously. NaDA was prepared from diisopropylamine, isoprene, DMEA, and sodium dispersion using a modified[7] procedure first reported by Wakefield.[5b] A precautionary crystallization was used for the work described herein. Solutions of NaDA were titrated using a literature method.[49] NaICA was prepared with an optimized dissolving-metal-based preparation analogous to that used to prepare NaDA.[7, 9a]

NaDCA.

NaDCA is more conveniently prepared using *n*-butylsodium[50] rather than sodium dispersion because of its lower solubility. To a dry 15 mL pear flask charged with *n*-butylsodium (33.0 mg, 0.413 mmol) was added DMEA (3.3 mL) at room temperature. On complete dissolution of the *n*-butylsodium, neat dicyclohexylamine (66.0 μL, 0.33 mmol) was added to provide a stock solution. ^{13}C NMR spectrum (125.72 MHz, DMEA) δ 61.9, 41.6, 27.3, 26.7; ^{15}N NMR spectrum (50.66 MHz, DMEA) 86.9.

NMR Spectroscopic Analyses.

NMR samples for reaction monitoring were routinely prepared using stock solutions of NaDA and sealed under partial vacuum. DMEA-free solutions of NaDA with added ligands used DMEA-free crystallized NaDA. Samples were routinely flame-sealed except when used in experiments involving serial titration with a coordinating ligand. Standard ^{1}H, ^{13}C, and ^{15}N spectra were recorded on a 500 MHz spectrometer at 500, 125.79, and 50.66 MHz, respectively. The ^{13}C, and ^{15}N resonances were referenced to the *C*H$_2$O resonance of THF at −90 °C (67.57 ppm), and neat Me$_2$NEt at −90 °C (25.7 ppm), respectively.

Supplementary Material

Refer to Web version on PubMed Central for supplementary material.

Acknowledgments.

References and Footnotes

1. Mulvey RE; Robertson SD Angew. Chem 2013, 52, 11470. [PubMed: 24133015]

2. Schlosser M In Organometallics in Synthesis : A Manual. Schlosser M, Ed.; Wiley: New York, 2002; Chapter 1.

3. (a) Bakker WII; Wong PL; Snieckus V. Lithium Diisopropylamide In e-EROS; Paquette LA, Ed.; Wiley: New York, 2001. (b) Clayden J Organolithiums: Selectivity for Synthesis; Baldwin JE, Williams RM, Eds.; Pergamon Press: New York, 2002. (c) Hartung CG; Snieckus V In Modern Arene Chemistry; Astruc D Ed.; Wiley- VCH, Weinheim, 2002; Chapter 10. (d) Collum DB; McNeil AJ; Ramírez A Angew. Chem., Int. Ed 2007, 46, 3002.

4. Raynolds S; Levine RJ Am. Chem. Soc 1959, 82, 472.

5. (a) Lochmann L; Trekoval JJ Organomet. Chem 1979, 179, 123. (b) Barr D; Dawson AJ; Wakefield BJJ Chem. Soc., Chem. Commun 1992, 204. (c) Lochmann L; Janata M Cent. Eur. J. Chem 2014, 12, 537.

6. (a) Munguia T; Bakir ZA; Cervantes-Lee F; Metta-Magana A; Pannell KH Organometallics 2009, 28, 5777. (b) Andrews PC; Barnett NDR; Mulvey RE; Clegg W; O'Neil PA; Barr D; Cowton L; Dawson AJ; Wakefield BJ J. Organomet. Chem 1996, 518, 85. (c) Boeckman RK; Boehmler DJ; Musselman RA Org. Lett 2001, 3, 3777. [PubMed: 11700136] (d) LaMontagne MP; Ao MS; Markovac A; Menke JR J. Med. Chem 1976, 19, 363. (e) Bond JL; Krottinger D; Schumacher RM; Sund EH; Weaver TJ J. Chem. Eng. Data 1973, 18, 349. (f) Levine R; Raynolds SJ Org. Chem 1960, 25, 530. (g) Mamane V; Louërat F; Iehl J; Abboud M; Fort Y Tetrahedron 2008, 64, 10699. (h) Baum BM; Levine RJ Heterocyclic Chem 1966, 3, 272. (i) Tsuruta T Makromol. Chem 1985, 13, 33.

7. Ma Y; Algera RF; Collum DB J. Org. Chem 2016, 81, 11312. [PubMed: 27768310]

8. (a) Renny JS; Tomasevich LL; Tallmadge EH; Collum DB Angew. Chem., Int. Ed 2013, 52, 11998. (b) Weingarten H; Van Wazer JR J. Am. Chem. Soc 1965, 87, 724. (c) Goralski P; Legoff D; Chabanel MJ Organomet. Chem 1993, 456, 1. (d) Goralski P; Chabanel M Inorg. Chem 1987, 26, 2169.

9. (a) Tomasevich LL; Collum DB J. Am. Chem. Soc 2014, 136, 9710. [PubMed: 24915602] (b) Liou LR; McNeil AJ; Ramírez A; Toombes GES; Gruver JM; Collum DB J. Am. Chem. Soc 2008, 130, 4859. [PubMed: 18336025]

10. Bartoň J; Kašpar M; Růžička V Collect. Czech. Chem. Commun 1982, 47, 594.

11. Kissling RM; Gagne MR J. Org. Chem 2001, 66, 9005. [PubMed: 11749634]

12. (a) Frisch MJ; et al. Gaussian 09, Revision A.02; Gaussian, Inc.: Wallingford, CT, 2009. (b) "Perspectives on Computational Organic Chemistry". Streitwieser A J. Org. Chem 2009 74, 4433. [PubMed: 19518150]

13. For a particularly incisive comparison of methods for calculating alkali metal solvation using both explicit and continuum models of solvation (including lithium and sodium solvated by THF and DME), see: Ziegler MJ; Madura JD J. Solution Chem 2011, 40, 1383.

14. Measuring the mole fraction within only the ensemble of interest rather than the overall mole fraction of NaDA added to the samples eliminates the distorting effects of impurities.

15. (a) Li D; Keresztes I; Hopson R; Williard PG Acc. Chem. Res 2009, 42, 270. [PubMed: 19105594] (b) Kagan G; Li L; Hopson R; Williard PG Org. Lett 2010, 12, 520. [PubMed: 20041695] (c) Su S; Hopson R; Williard PG J. Org. Chem 2013, 78, 11733. [PubMed: 24134615] (d) Guang J; Hopson R; Williard PG J. Org. Chem 2015, 80, 9102. [PubMed: 26318438] (e) Guang J; Liu QP; Hopson R; Williard PG J. Am. Chem. Soc 2015, 137, 7347. [PubMed: 25933508] (f) Su G; Guang J; Li W; Wu K; Hopson R; Williard PG J. Am. Chem. Soc 2014, 136, 11735. [PubMed: 25053148]

16. (a) Armstrong DR; Harris CMM; Kennedy AR; Liggat JJ; McLellan R; Mulvey RE; Urquhart MDT; Robertson SD Chem.–Euro. J 2015, 21, 14410. (b) Neufeld R; John M; Stalke D Angew. Chem., Int. Ed 2015, 54, 6994. (c) Hamdoun G; Sebban M; Cossoul E; Harrison-Marchand A; Maddaluno J; Oulyadi H Chem. Commun 2014, 50, 4073. (d) Armstrong DR; Garden JA; Kennedy AR; Leenhouts SM; Mulvey RE; O'Keefe P; O'Hara CT; Steven A Chem.–Euro. J 2013, 19, 13492. (e) Lecachey B; Duguet N; Oulyadi H; Fressigne C; Harrison-Marchand A; Yamamoto Y; Tomioka K; Maddaluno J Org. Lett 2009, 11, 1907. [PubMed: 19358566]

17. DOSY has been used to study sodium 2,2,6,6-tetramethylpiperidide: Armstrong R; Garcia-Alvarez P; Kennedy AR; Mulvey RE; Robertson SD Chem. Eur. J 2011, 17, 6725. [PubMed: 21538621]

18. (a) Bloor EG; Kidd RG Can. J. Chem 1968, 46, 3425. (b) Erlich RH; Popov AI J. Am. Chem. Soc 1971, 93, 5620. (c) Arnett EM; Ko HC; Minasz RJ J. Phys. Chem 1972, 76, 2474. (d) Herlem M; Popov AI J. Am. Chem. Soc 1972, 94, 1431. (e) Kintzinger JP; Lehn JM J. Am. Chem. Soc 1974, 96, 3313. (f) Van Geet AL J. Am. Chem. Soc 1972, 94, 5583. (g) Templeman GJ; Van Geet AL J. Am. Chem. Soc 1972, 94, 5578.

19. (a) Cheema ZW; Gibson GW; Eastham JF J. Am. Chem. Soc 1963, 85, 3517. (b) Eastham JF; Gibson GW J. Am. Chem. Soc 1963, 85, 2171. (c) Settle FA; Haggerty M; Eastham JF J. Am. Chem. Soc 1964, 86, 2076. (d) Waack R Doran MA; Stevenson PE J. Am. Chem. Soc 1966, 88, 2109. (e) Bartlett PD; Goebel CV; Weber WP J. Am. Chem. Soc 1969, 91, 7425. (f) Lewis HL; Brown TL J. Am. Chem. Soc 1970, 92, 4664. (g) Popov AI Pure Appl. Chem 1975, 41, 275. (h) Sergutin VM; Zgonnik VN; Kalninsh KK J. Organomet. Chem 1979, 170, 151. (i) Kminek; Kaspar M; Trekoval J Coll. Czech. Chem. Commun 1981, 1132. (j) Sunner J; Kebarle P J. Am. Chem. Soc 1984, 106, 6135. (k) Wanat RA; Collum DB; Van Duyne G; Clardy J; DePue RT J. Am. Chem. Soc 1986, 108, 3415. (l) Kallman N; Collum DB J. Am. Chem. Soc 1987, 109, 7466.

20. The value of n is preset to give an analytically solvable form to which the data can be fitted explicitly.

21. Collum DB Acc. Chem. Res 1993, 26, 227.

22. Monodentate TMEDAs on lithium are common. For recent examples, see: Jin KJ; Collum DB J. Am. Chem. Soc 2015, 137, 14446. [PubMed: 26554898] Zhang S; Zhan M; Zhang W-X; Xi Z Organometallics 2013, 32, 4020. Aharonovich S; Botoshanski M; Rabinovich Z; Waymouth RM; Eisen MS Inorg. Chem 2010, 49, 1220. [PubMed: 20039691] Andrews PC; Koutsaplis M; Robertson EG Organometallics 2009, 28, 1697. Clegg W; Graham DV; Herd E; Hevia E; Kennedy AR; McCall MD; Russo L Inorg. Chem 2009, 48, 5320. [PubMed: 19408922]

23. Sodium coordinated by an η^1-TMEDA: Kennedy AR; Mulvey RE; O'Hara CT; Robertson SD; Robertson GM Acta Crystallogr., Sect. E: Struct. Rep. Online 2012, 68, m1468.

24. Monodentate DMEs on lithium are common. For recent examples, see: Majumdar M; Omlor I; Yildiz B; Azizoglu A; Huch V; Scheschkewitz D Angew. Chem., Int. Ed 2015, 54, 8746. Schowtka B; Gorls H; Westerhausen MZ Anorg. Allg. Chem 2014, 640, 907. Seo DM; Boyle PD; Allen JL; Han S-D; Jonsson E; Johansson P; Henderson WA J. Phys. Chem. C 2014, 118, 18337. Ren W; Deng X; Zi G; Fang D-CJ Chem. Soc., Dalton Trans 2011, 40, 9662. Beck JF; Neshat A; Schmidt JA R. Eur. J. Inorg. Chem 2010, 5146. Lewis RA; Wu G; Hayton TW J. Am. Chem. Soc 2010, 132, 12814. [PubMed: 20735123] Volpe EC; Manke DR; Bartholomew ER; Wolczanski PT; Lobkovsky EB Organometallics 2010, 29, 6642.

25. Sodium coordinated by an η^1-DME: Gallo E; Solari E; Floriani C; Chiesi-Villa A; Rizzoli C Inorg. Chem 1997, 36, 2178. [PubMed: 11669841]

26. (a) Ali A; Langer M; Lorenz V; Hrib CG; Hilfert L; Edelmann FT J. Organomet. Chem 2015, 776, 163. (b) Al-Harbi A; Rong Y; Parkin G Inorg. Chem 2013, 52, 10226. [PubMed: 23987579] (c) Neander S; Kornich J; Olbrich F J. Organomet. Chem 2002, 656, 89. (d) Bock H; Gharagozloo-Hubmann K; Holl S; Sievert MZ Naturforsch., B: Chem. Sci 2000, 55, 1163. (e) Bock H; Arad C; Nather CJ Organomet. Chem 1996, 520, 1. (f) Bock H; Arad C; Nather C; Gobel I; John AZ Naturforsch., B: Chem. Sci 1996, 51, 1391. (g) Bock H; Arad C; Nather C; Gobel I Helv. Chim. Acta 1996, 79, 92. (h) Gallo E; Solari E; De Angelis S; Floriani C; Re N; Chiesi-Villa A; Rizzoli CJ Am. Chem. Soc 1993, 115, 9850. (i) Mulvey RE; Clegg W; Barr D; Snaith R Polyhedron 1986, 5, 2109.

27. There are approximately a dozen instances in which PMDTA binds as a bidentate rather than the highly preferred tridentate motif: Armstrong DR; Brouillet EV; Kennedy AR; Garden JA; Granitzka M; Mulvey RE; Trivett JJ J. Chem. Soc., Dalton Trans 2014, 43, 14409.

28. (a) Titration of a NaDA suspension with *trans-N,N,N',N'-*tetramethylcyclohexanediamine (TMCDA) shows a linear dependence of the titer on TMCDA with a hard solubility endpoint at a 2:1 stoichiometry, which contrasts with the 1:1 proportions for TMEDA (supporting information). MCV did not reveal spectral distortions consistent with heteroaggregation when paired with NaICA, which implicated a doubly chelated monomer.[28b] However, preliminary rate data on a metalation (unpublished) suggested a fractional-order dependence on NaDA, which argues for a

requiste dimer deaggregation. η²-TMCDA on sodium:(b) TMCDA-solvated LDA in hydrocarbons is monomeric: Remenar JF; Lucht BL; Collum DB J. Am. Chem. Soc 1997, 119, 5567. Ojeda-Amador AI; Martinez-Martinez AJ; Kennedy AR; Armstrong DR; O'Hara CT Chem. Commun 2017, 53, 324. Garcia-Alvarez P; Kennedy AR; O'Hara CT; Reilly K; Robertson GMJ Chem. Soc., Dalton Trans 2011, 40, 5332.

29. (a) Mukhopadhyay T; Seebach D Helv. Chim. Acta 1982, 65, 385. (b) Sun X; Collum DB J. Am. Chem. Soc 2000, 122, 2459.

30. (a) Melchior MT; Klemann LP; Whitney TA; Langer AW, Jr. Am. Chem. Soc., Polym. Preprints 1972, 13, 649. (b) Koehler FH; Hertkorn N; Bluemel J Chem. Ber 1987, 120, 2081. (c) Bates RB; Kroposki LM; Potter DE J. Org. Chem 1970, 37, 560. Stanetty P; Koller H; Mihovilovic M J. Org. Chem 1992, 57, 6833. (d) Melchior MT; Klemann LP; Whitney TA; Langer AW, Jr. Am. Chem. Soc., Polym. Preprints 1972, 13, 649. (e) Koehler FH; Hertkorn N; Bluemel J Chem. Ber 1987, 120, 2081. (f) Kopka IE; Fataftah ZA; Rathke MW J. Org. Chem 1987, 52, 448.

31. Studies of base-mediated solvent decomposition: Holm T Acta Chem. Scand 1978, 32B, 162. Bates TF; Clarke MT; Thomas RD J. Am. Chem. Soc 1988, 110, 5109. Raposo ML; Fernández-Nieto F; Garcia-Rio L; Rodríguez-Dafonte P; Paleo MR; Sardina FJ Chem. Eur. J 2013, 19, 9677. [PubMed: 23740791] Corset J; Castellà-Ventura M; Froment F; Strzalko T; Wartski LJ Raman Spectrosc 2002, 33, 652.

32. We occasionally turn to a method based on a nonlinear least-squares fit to the non-linear variant[32a] of the Noyes equation:[32b]

$$[substrate] \ = \ \left\{ (n-1)k_{obsd}t \ + \ [substrate]_0^{(1-n)} \right\}^{1/(1-n)}$$

The adjustable parameter n corresponds to the reaction order in the decaying substrate. Briggs TF; Winemiller MD; Collum DB; Parsons RL, Jr.; Davulcu AK; Harris GD; Fortunak JD; Confalone PN J. Am. Chem. Soc 2004, 126, 5427. [PubMed: 15113214] Noyes AA Am. Chem. J 1897, 19, 766.

33. We define the idealized rate law as that obtained by rounding the observed reaction orders to the nearest rational order.

34. The rate law provides the stoichiometry of the transition structure relative to that of the reactants: Edwards JO; Greene EF; Ross J J. Chem. Educ 1968, 45, 381.

35. Leading references to oxacarbenoids: Boche G; Lohrenz JCW. Chem Rev 2001, 101, 697. [PubMed: 11712501] Boche G; Bosold F; Lohrenz JCW; Opel A; Zulauf P Chem. Ber 1993, 126, 1873. Baumgartner T; Gudat D; Nieger M; Niecke E; Schiffer TJ J. Am. Chem. Soc 1999, 121, 5953.

36. (a) Bissell ER; Finger M J. Org. Chem 1959, 24, 1259. (b) Yang YK; Bergman RG Organometallics 1985, 4, 129.

37. There are an enormous number of documented $^+Na(THF)_6$ and $^+Na(\eta^2\text{-DME})_3$ gegenions. For an example of both see: Livingstone Z; Hernan-Gomez A; Baillie SE; Armstrong DR; Carrella LM; Clegg W; Harrington RW; Kennedy AR; Rentschler E; Hevia EJ Chem. Soc., Dalton Trans 2016, 45, 6175.

38. For an example and extensive leading references to applications of simple (monofunctional) trialkylamines in organolithium chemistry, see: Godenschwager P; Collum DB J. Am. Chem. Soc 2008, 130, 8726. [PubMed: 18557616]

39. Williard PG; Salvino JM J. Org. Chem 1993, 58, 1.

40. Hoepker AC; Collum DB J. Org. Chem 2011, 76, 7985. [PubMed: 21888365]

41. Manifestation of a steric effect as an entropic contribution has been referred to as "population control".[42a] Previous authors have concluded that differences in penchants for ion solvation stem from entropic effects.[42b,c]

42. (a) Winans RE; Wilcox CF, Jr. J. Am. Chem. Soc 1976, 98, 4281. (b) Lucht BL; Collum DB J. Am. Chem. Soc 1995, 117, 9863. (c) Strong J; Tuttle TR, Jr. J. Phys. Chem 1973, 77, 533.

43. It may be instructive for some to note that simple thermochemical expression, $\Delta G = \Delta H - T\Delta S$, seems to bait many into believing that the temperature dependence of an equilibrium (or any ratio of relative rates) is inherently entropic. However, when combined with a second thermochemical cornerstone, $\Delta G = -RT\ln K_{eq}$, we find that $\ln K_{eq} = -\Delta H/RT + \Delta S/R$. We see that the existence

and direction of a temperature dependence derives exclusively from the enthalpic term. A species is promoted by lowering the temperature if and only if it is enthalpically preferred.

44. Ramírez A; Sun X; Collum DB J. Am. Chem. Soc 2006, 128, 10326 and references cited therein. [PubMed: 16881665]

45. (a) Angell SE; Rogers CW; Zhang Y; Wolf MO; Jones WE Coord. Chem. Rev 2006, 250, 1829. (b) Braunstein P; Naud F Angew. Chem., Int. Ed 2001, 40, 680 (c) Slone CS; Weinberger DA; Mirkin CA Progr. Inorg. Chem 1999, 48, 233.

46. Ma Y; Hoepker AC; Gupta L; Faggin MF; Collum DB J. Am. Chem. Soc 2010, 132, 15610. [PubMed: 20961095]

47. Aubrecht KB; Collum DB J. Org. Chem 1996, 61, 8674.

48. Galiano-Roth AS; Michaelides EM; Collum DB J. Am. Chem. Soc 1988, 110, 2658.

49. Kofron WG; Baclawski LM J. Org. Chem 1976, 41, 1879.

50. Lochmann L; Pospisil J; Lim D Tetrahedron Lett 1966, 7, 257.
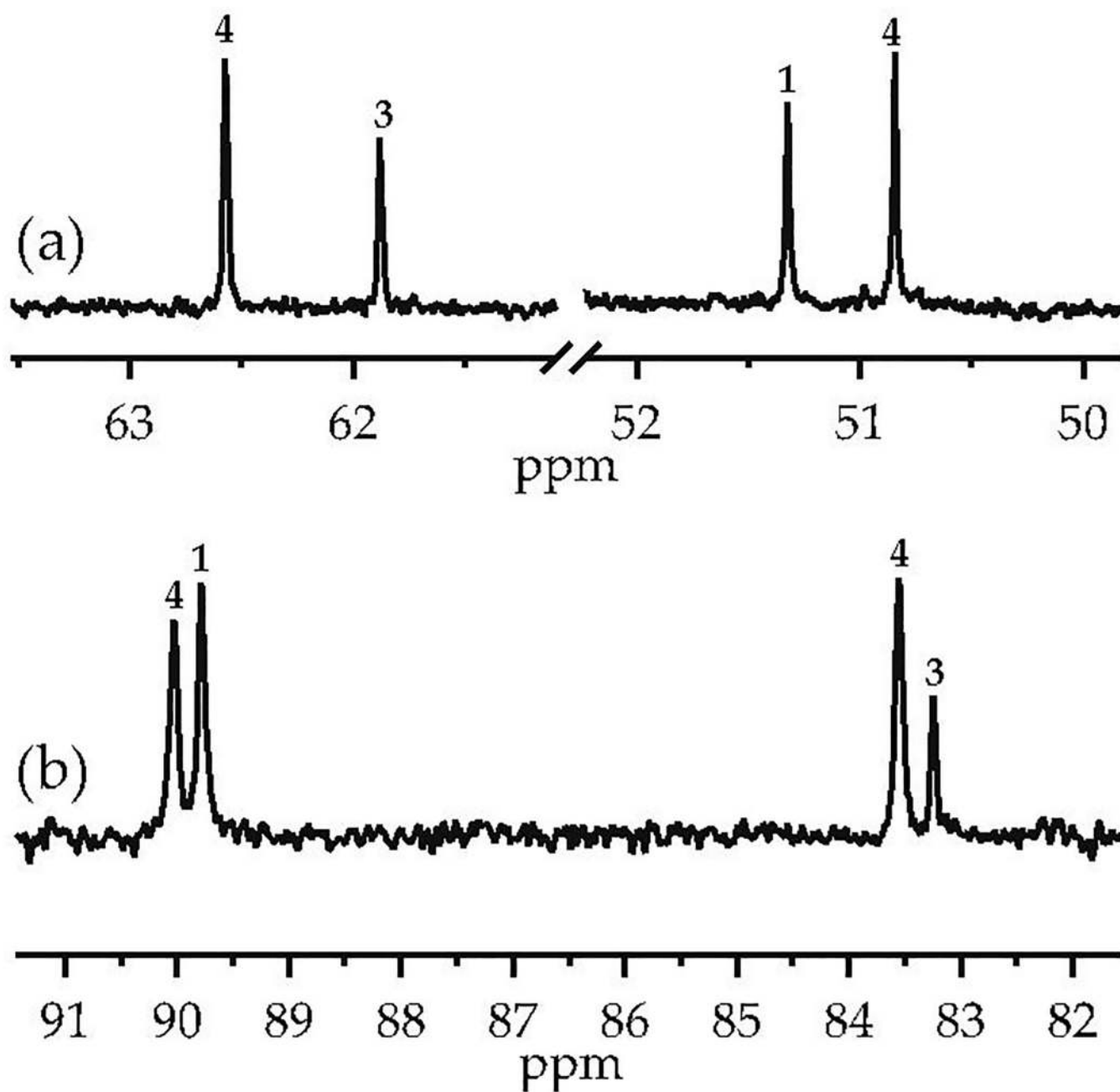
Figure 1.
NMR spectra of a ~1:1 mixture (0.10 M total titer) of sodium diisopropylamide (NaDA; **1**) and sodium dicyclohexylamide (NaDCA; **3**) in neat dimethylethylamine (DMEA) affording heterodimer **4**. (a) ^{13}C NMR spectrum recorded at −80 °C; (b) ^{15}N NMR spectrum using [^{15}N]NaDA and [^{15}N]NaDCA recorded at −100 °C.
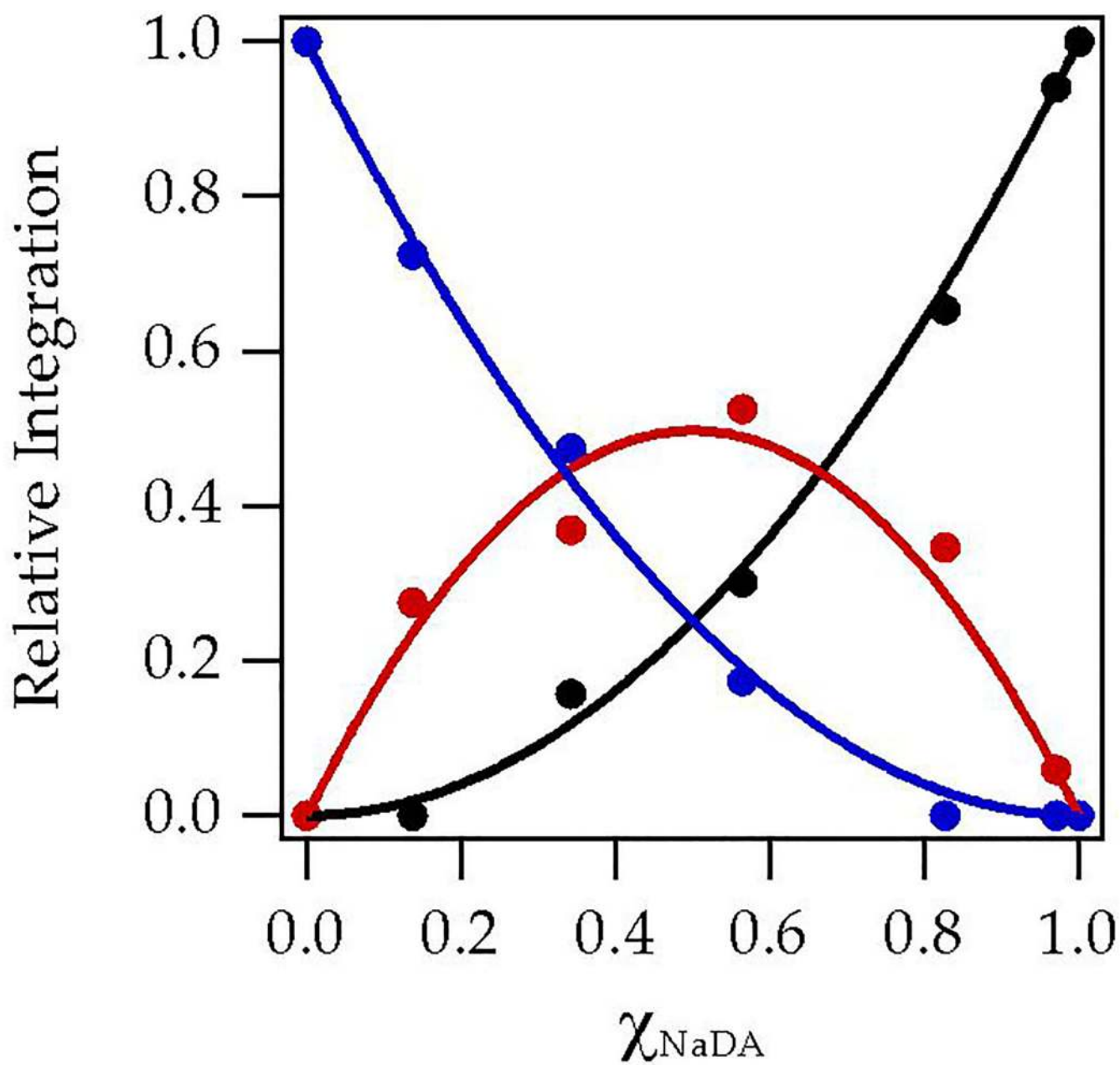
Figure 2.
Job plot showing relative integrations of the ^{13}C resonances of **1** (black), **3** (blue), and **4** (red) versus the measured[14] mole fraction of NaDA (X_{NaDA}) for mixtures of NaDCA and NaDA in neat DMEA at −80 °C.
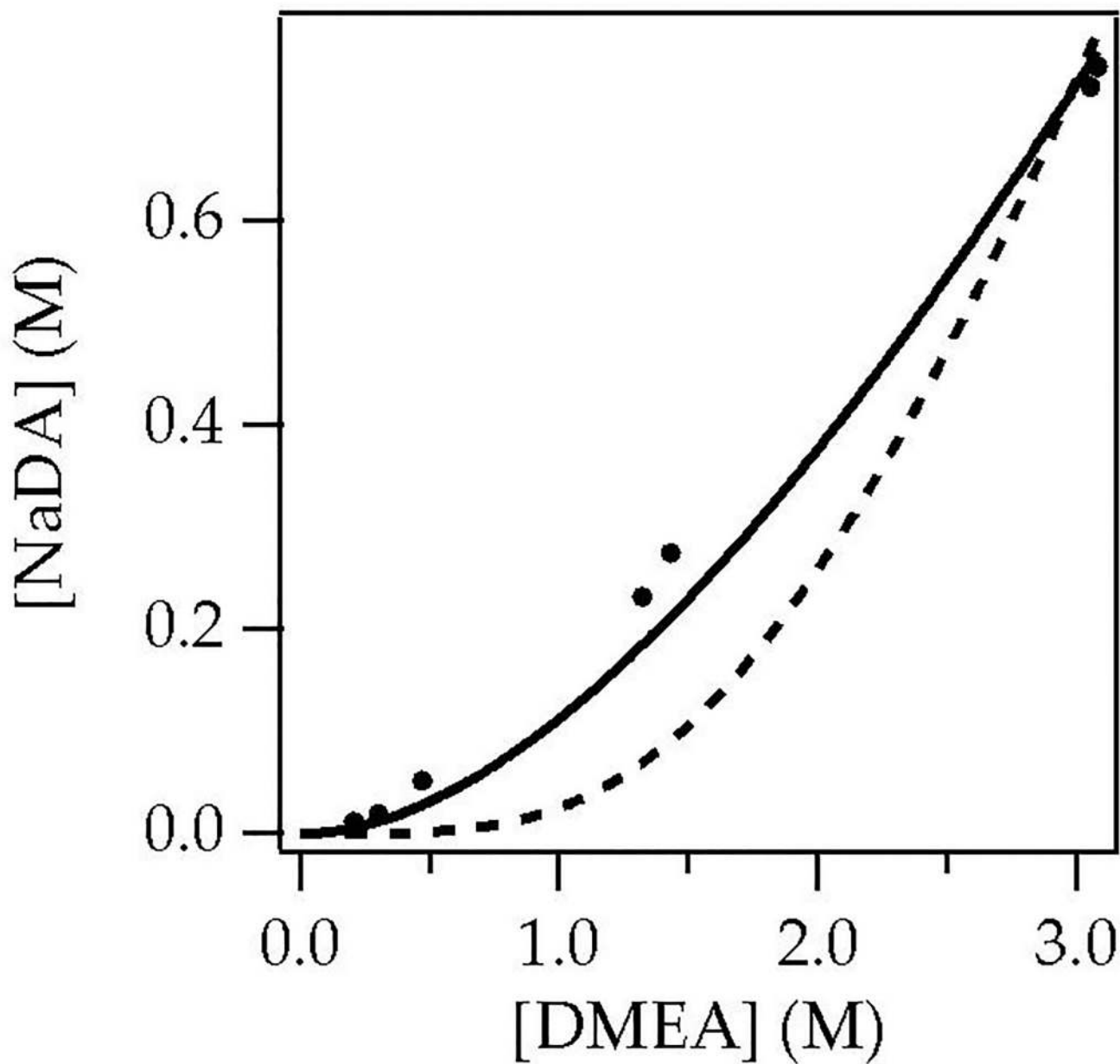
Figure 3.
Plot of NaDA concentration versus total DMEA concentration in toluene at room temperature fit to equation 7 and presuming one DMEA per sodium (solid line, $n = 2$ [set],[20] $K_{solv} = 0.072 \pm 0.004$) and two DMEA per sodium (dashed line, $n = 4$ [set], $K_{solv} = 0.007 \pm 0.002$).
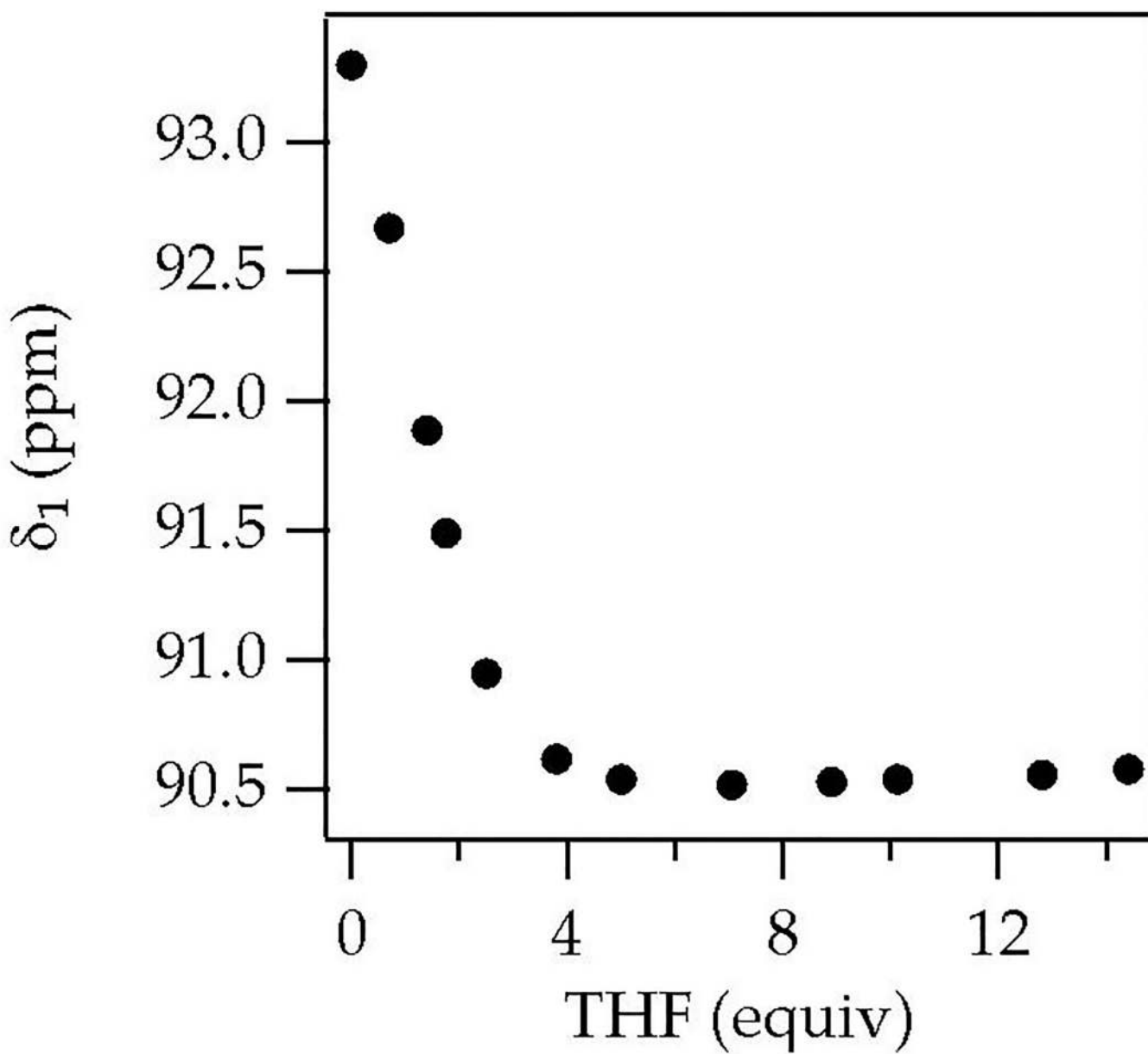
Figure 4.
Plot of ^{15}N chemical shifts of **1** versus equivalents of tetrahydrofuran (THF) in 2.0 M DMEA–hexane at −80 °C.
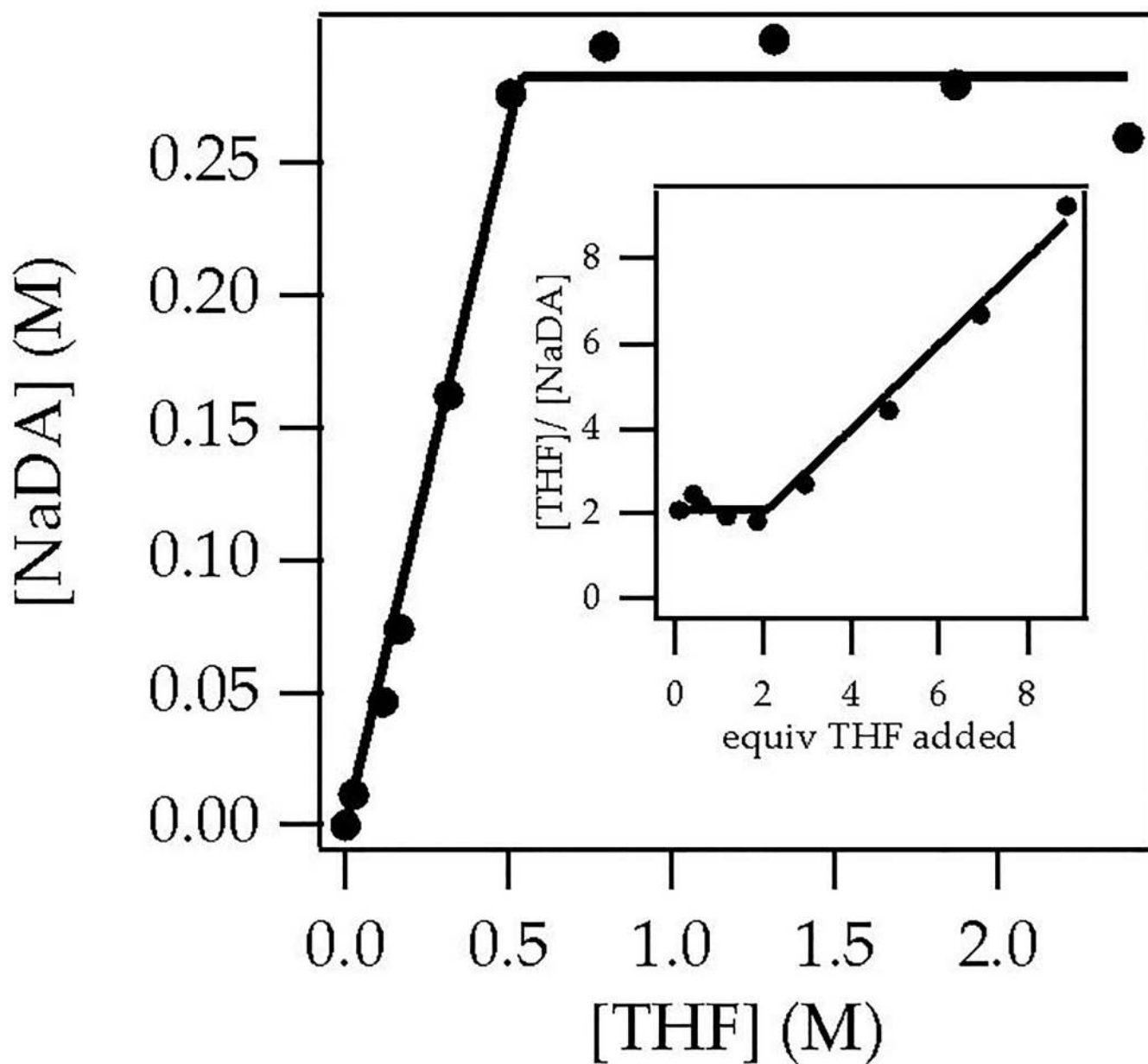
Figure 5.
Plot of NaDA concentration versus total THF concentration for suspensions of NaDA in toluene at room temperature. The concentration is measured relative to benzene (internal standard). Inset: Plot of THF/NaDA concentration versus equivalents of THF added to the anticipated amount of NaDA at room temperature. The discontinuities correspond to full solubilization.
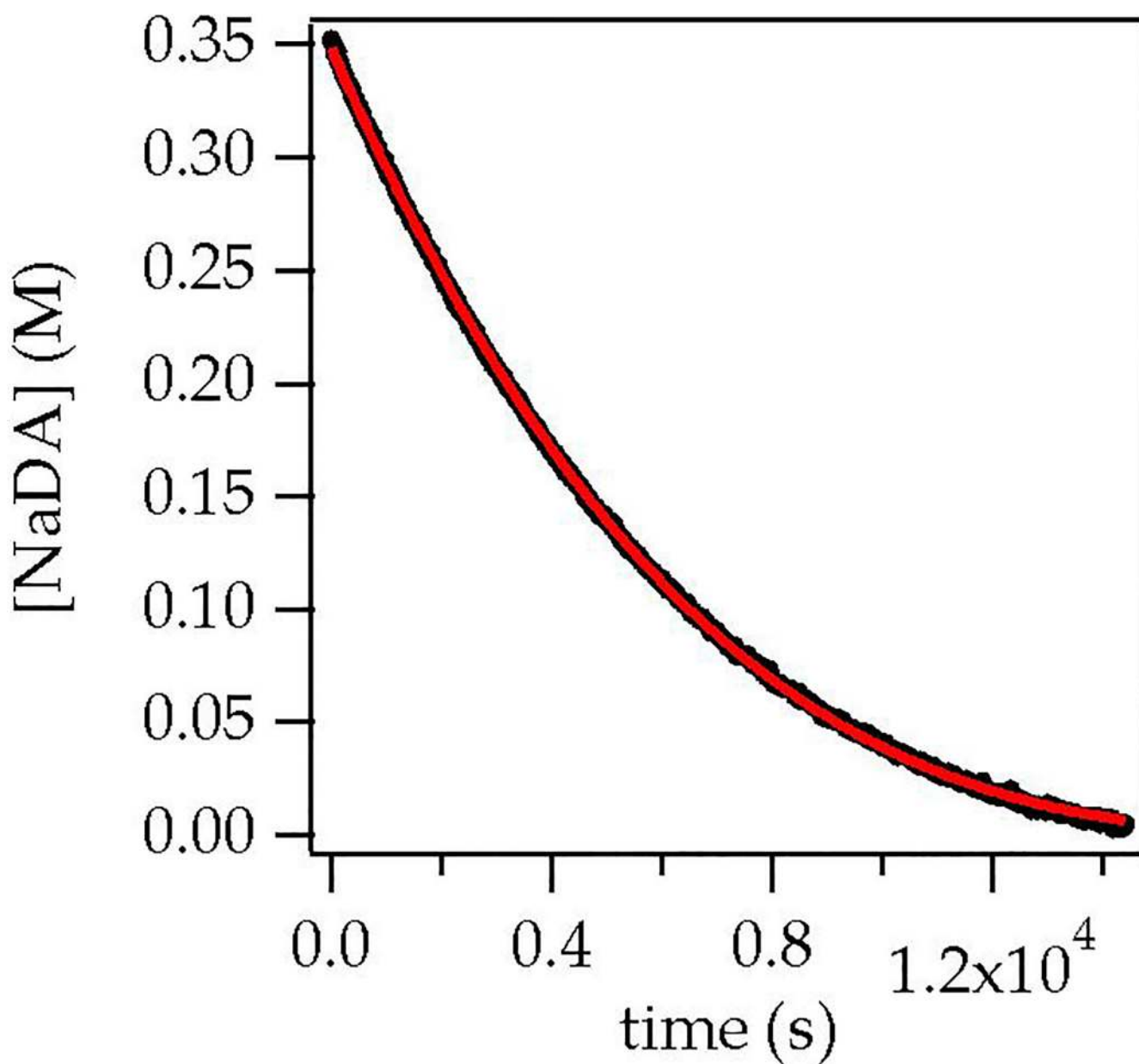
Figure 6.
Plot of NaDA concentration versus time for the decomposition of THF (Scheme 1) of NaDA at 25 °C. The red curve depicts an unweighted least-squares fit to the function $f(t) = [a^{1-n} - kt/(1-n)]^{[1/(1-n)]}$: $a = 0.3484 \pm 0.0002$; $k = 1.061 \times 10^{-5} \pm 9 \times 10^{-8}$; $n = 0.698 \pm 0.002$.
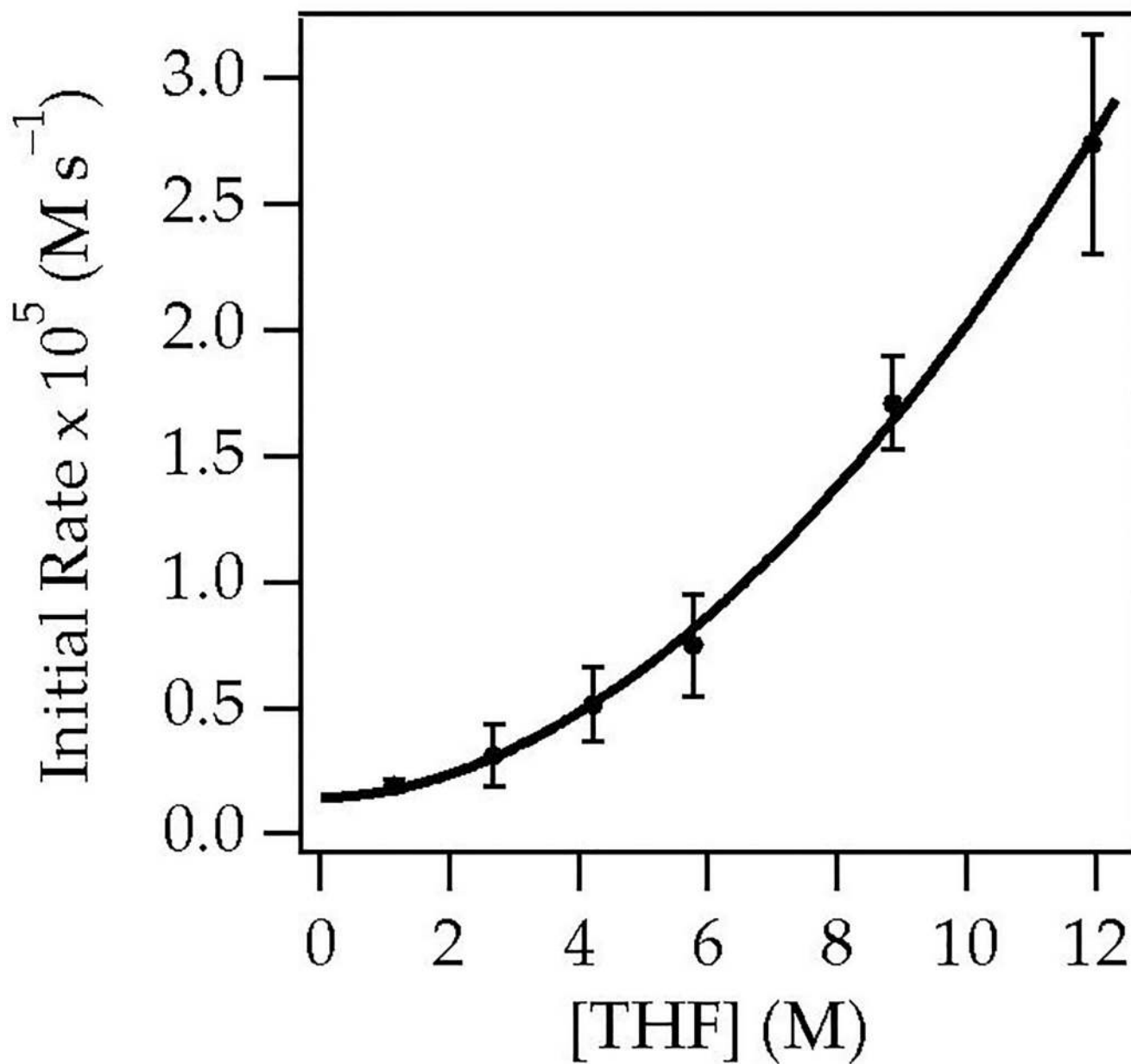
Figure 7.
Plot of initial rates versus THF concentration for the decomposition of THF (Scheme 1) in 0.20 M NaDA at 25 °C. The curve depicts an unweighted least-squares fit to the function $f(\mathrm{x}) = ax^b + c$: $a = 0.025 \pm 0.008$; $b = 1.9 \pm 0.1$; $c = 0.14 \pm 0.05$.
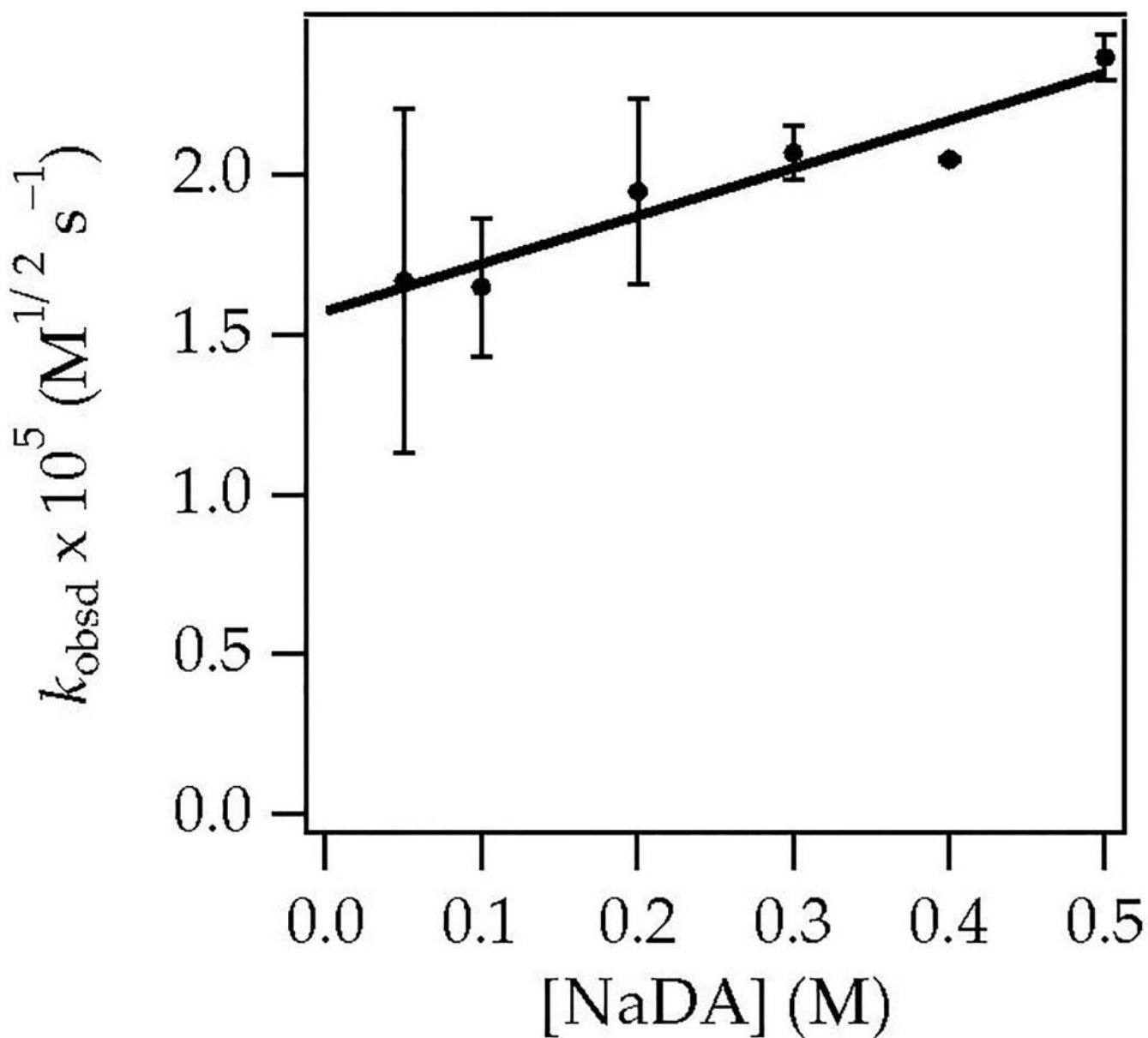
Figure 8.
Plot of pseudo-*half*-order rate constants (k_{obsd}) versus NaDA concentration for the decomposition of THF (Scheme 1) in neat THF at 25 °C. The curve depicts an unweighted least-squares fit to the function $f(x) = ax + b$: $a = 1.5 \pm 0.2$; $b = 1.57 \pm 0.07$.
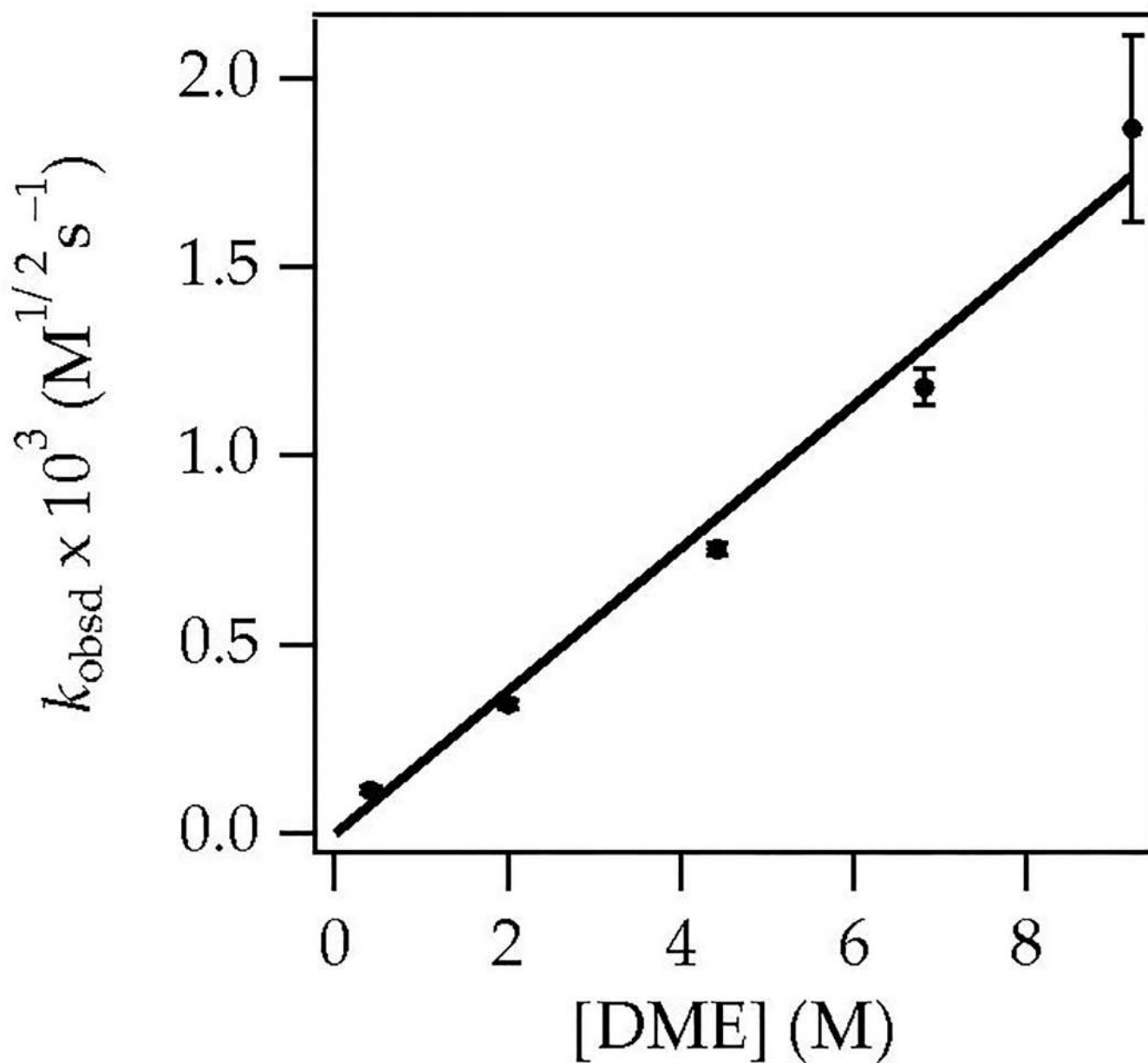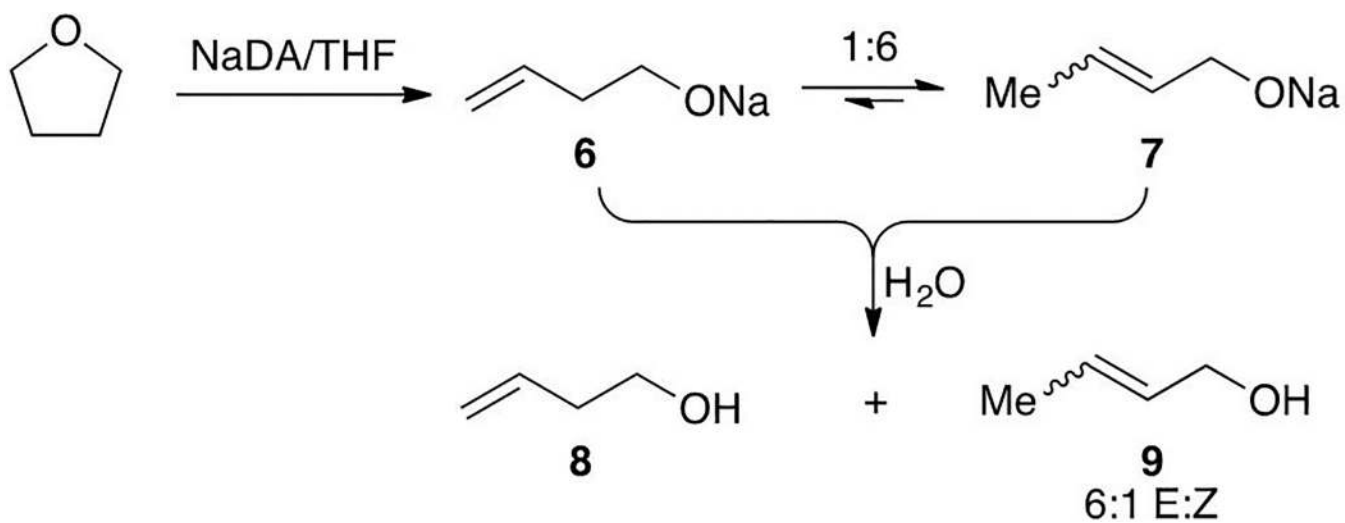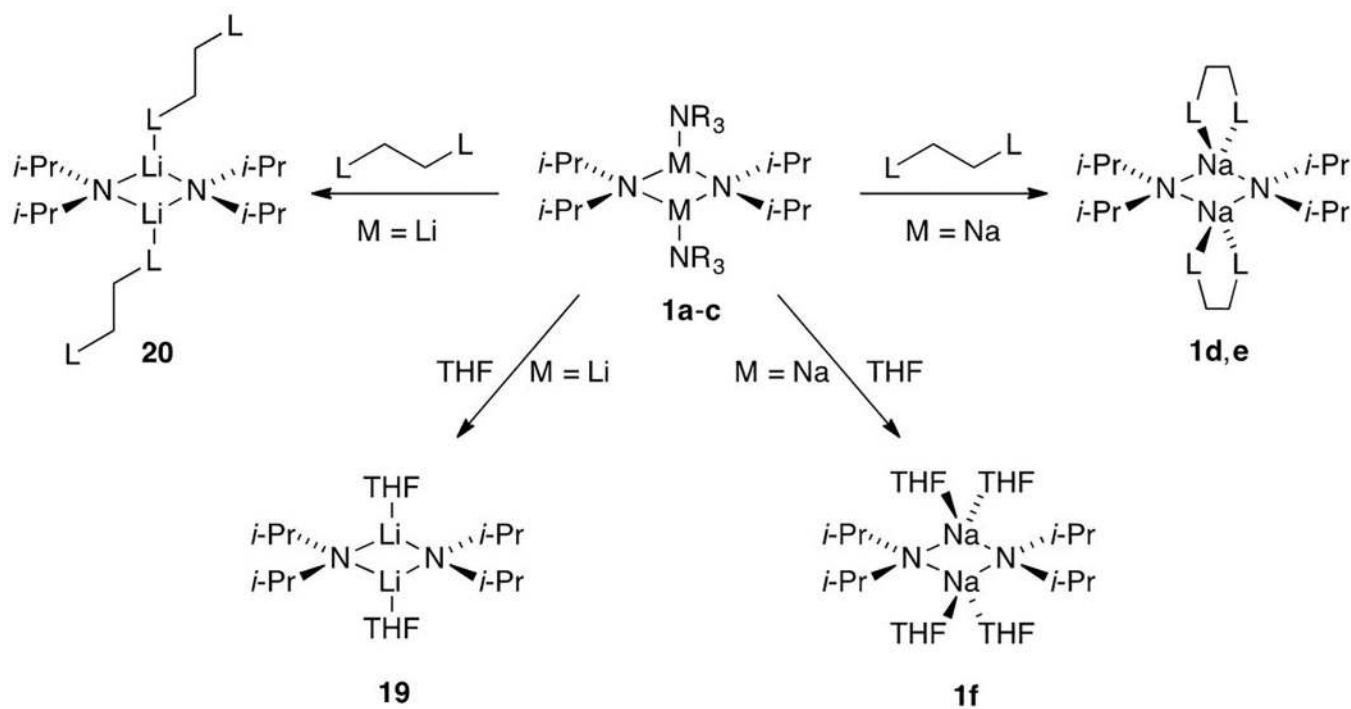
Figure 9.
Plot of k_{obsd} versus dimethoxyethane (DME) concentration for the decomposition of DME (eq 12) in 0.40 M NaDA at −10 °C. The curve depicts an unweighted least-squares fit to the function $f(x) = ax$: $a = 0.189 \pm 0.008$.

Scheme 1.
Decomposition of THF

Scheme 2.
Mechanism of THF Decomposition

Scheme 3.
Comparison of NaDA and LDA Structures.

Table 1.

Molecular Weight (MW) of Sodium Diisopropylamide in Dimethylethylamine and Tetrahydrofuran Determined with [1]H Diffusion-Ordered Spectroscopy

Aggregate	Calculated MW	Diffusion MW (–80 °C)	Diffusion MW (rt)
1a	393	298	391
1f	534	565	481

rt, room temperature.

Table 2:

Approximate Half-Life of 0.30 M NaDA in Common Laboratory Solvents at Room Temperature

Ligand[a]	Half-life
DMEA	2 months
TMEDA	1 month
THF	1 h
DME	10 s
DMPU[b]	<<1 s

[a]Neat.

[b]0.30 M DMPU in DMEA.